New Phytologist

Research

Methods

Targeted CRISPR-Cas9-based gene knockouts in the model brown alga *Ectocarpus*

Yacine Badis[1,2], Delphine Scornet[1], Minori Harada[3], Céline Caillard[1], Olivier Godfroy[1], Morgane Raphalen[1], Claire M. M. Gachon[2,4], Susana M. Coelho[1,5], Taizo Motomura[6], Chikako Nagasato[6] and J. Mark Cock[1]

[1]Roscoff Biological Station, Place Georges Teissier, Roscoff 29680, France; [2]The Scottish Association for Marine Science, Scottish Marine Institute, Oban, Argyll, PA37 1QA, UK; [3]Graduate School of Environmental Science, Hokkaido University, Sapporo 060-0810, Japan; [4]UMR 7245 Molécules de Communication et Adaptation des Micro-organismes, Muséum National d'Histoire Naturelle, CP 54, 57 rue Cuvier, Paris 75005, France; [5]Department of Algal Development and Evolution, Max Planck Institute for Developmental Biology, Max-Planck-Ring 5, Tübingen 72076, Germany; [6]Muroran Marine Station, Field Science Center for Northern Biosphere, Hokkaido University, Muroran 051-0013, Japan

Author for correspondence:
Yacine Badis
Email: yacine.badis@sams.ac.uk

Received: *2 December 2020*
Accepted: *20 May 2021*

New Phytologist (2021) **231:** 2077–2091
doi: 10.1111/nph.17525

Key words: brown alga, Cas9, CRISPR, *Ectocarpus*, reverse genetics, transformation.

Summary

- Brown algae are an important group of multicellular eukaryotes, phylogenetically distinct from both the animal and land plant lineages. *Ectocarpus* has emerged as a model organism to study diverse aspects of brown algal biology, but this system currently lacks an effective reverse genetics methodology to analyse the functions of selected target genes.
- Here, we report that mutations at specific target sites are generated following the introduction of CRISPR-Cas9 ribonucleoproteins into *Ectocarpus* cells, using either biolistics or microinjection as the delivery method.
- Individuals with mutations affecting the *ADENINE PHOSPHORIBOSYL TRANSFERASE* (*APT*) gene were isolated following treatment with 2-fluoroadenine, and this selection system was used to isolate individuals in which mutations had been introduced simultaneously at *APT* and at a second gene. This double mutation approach could potentially be used to isolate mutants affecting any *Ectocarpus* gene, providing an effective reverse genetics tool for this model organism.
- The availability of this tool will significantly enhance the utility of *Ectocarpus* as a model organism for this ecologically and economically important group of marine organisms. Moreover, the methodology described here should be readily transferable to other brown algal species.

Introduction

Brown seaweeds (i.e. algae of the class Phaeophyceae) are currently attracting considerable interest for both fundamental and applied research. Features of fundamental interest include their complex life cycles and the fact that they have evolved complex multicellular development independently of other major lineages, such as animals and land plants (Coelho & Cock, 2020). From an applied point of view, their evolutionary history as part of the stramenopile group has also been important, resulting in the emergence of a diverse range of unique algal metabolites (McHugh, 2003). Brown algae also play important ecological roles (Klinger, 2015). They are often the predominant primary producers in rocky shore ecosystems, providing habitats for other species and making an important contribution to global carbon (C) sequestration (Ortega *et al.*, 2019). Given their key ecological role, it is also important to understand brown algal biology in order to address current environmental challenges resulting from the unprecedented pace of global warming. Seaweeds have the capacity to significantly mitigate climate change through C sequestration (Chung *et al.*, 2011; Duarte *et al.*, 2017), but, at the same time, changes to the coastal environments threaten the resilience of natural seaweed populations (Wahl *et al.*, 2015; Coleman & Wernberg, 2017; Coleman & Goold, 2019).

Within the brown algae, members of the Ectocarpales have several features, such as short life cycles, small size at maturity, and small genome sizes, that make them well adapted for genetic studies. One member of this order, the filamentous brown alga *Ectocarpus siliculosus* (currently referred to as *Ectocarpus* species 7, see the Materials and Methods section for further details), was proposed as a model species in 2004 (Peters *et al.*, 2004). A broad range of tools and resources were subsequently established for this organism, including the complete sequence of its genome (the first to be sequenced for a macroalga; Cock *et al.*, 2010; Cormier *et al.*, 2017), stramenopile-adapted bioinformatics tools (Gschloessl *et al.*, 2008), microarrays and RNA-sequencing-based transcriptomic data, the latter for both protein-coding and noncoding genes (Dittami *et al.*, 2009; Ritter *et al.*, 2014;

Lipinska *et al.*, 2015; Tarver *et al.*, 2015; Strittmatter *et al.*, 2016; Cormier *et al.*, 2017), and proteomic (Ritter *et al.*, 2010) and epigenetic methodologies (Bourdareau *et al.*, 2021). In addition, genetic tools have been established, including sequence-tagged genetic maps (Heesch *et al.*, 2010; Avia *et al.*, 2017), mutant collections, and forward genetic screens (Godfroy *et al.*, 2017; Macaisne *et al.*, 2017; Arun *et al.*, 2019). These resources have been used to investigate diverse aspects of brown algal biology, and *Ectocarpus* species 7 is currently the most intensely studied species within the brown algae. Recent advances include the identification of quantitative genetic loci associated with adaptation to environmental stresses (Avia *et al.*, 2017) and the identification of genes that act as master regulators of the life cycle (Arun *et al.*, 2019) or that play important roles in other developmental processes (Godfroy *et al.*, 2017; Macaisne *et al.*, 2017).

These studies have illustrated the potential of *Ectocarpus* species 7 as a model system. However, although important advances have been made, the absence of a reverse genetics tool for this organism remains an important constraint, limiting the scope of functional approaches that can be applied. Indeed, the absence of a genetic transformation system has been repeatedly highlighted as an important bottleneck for brown algal research (Kroth, 2013; Mikami, 2014). A protocol for stable plasmid-based transformation has been recently developed for the green macroalga *Ulva mutabilis* (Oertel *et al.*, 2015), and there have been reports of transient expression of transgenes in red macroalgae (Hirata *et al.*, 2011; Mikami, 2014). For brown algae, earlier studies reported transient expression (Jiang *et al.*, 2003) and stable integration (Zhang *et al.*, 2008) of foreign genes in the kelp *Saccharina* (formerly *Laminaria*) *japonica*, but to date these methods have not been replicated nor widely adopted by the phycological community. An alternative approach, involving injection of double-stranded RNA has been shown to induce RNA-interference-based gene silencing in *Fucus serratus* embryos (Farnham *et al.*, 2013), and a modification of this protocol based on transfection of small interfering RNAs into gametes has been used to investigate gene function during early development of *Ectocarpus* species 7 partheno-sporophytes (Godfroy *et al.*, 2017; Macaisne *et al.*, 2017). However, RNA interference is still very inefficient in *Ectocarpus* species 7, affecting only a small proportion of the transfected cells, and is only applicable for genes that have phenotypes very early during development.

CRISPR-Cas9 is a bacteria-derived ribonucleoprotein (RNP) complex that uses a sequence-specific guide RNA (gRNA) to detect and cut sites complementary to the gRNA in DNA. CRISPR-Cas9-based approaches have been used successfully to induce targeted mutations in the genomes of several unconventional model organisms, including oomycetes (Fang *et al.*, 2017) and diatoms (Nymark *et al.*, 2016), which, like the brown algae, are members of the stramenopile lineage. Deployment of CRISPR-Cas9 in oomycetes and diatoms used pre-existing DNA transformation protocols, an approach that is currently unavailable for brown algae. In contrast, direct delivery of CRISPR-Cas9 RNPs, as first demonstrated in *Caenorhabditis elegans* (Cho *et al.*, 2013) does not require the existence of a transformation protocol and this approach could therefore be potentially applied to brown algal models. Direct delivery of CRISPR-Cas9 RNPs has been recently adapted for the model diatom *Phaeodactylum tricornutum* to target endogenous counter-selectable marker genes, resulting in a DNA-free gene knock-out system (Serif *et al.*, 2018). The latter study notably targeted the *Adenine Phosphoribosyl Transferase* (*APT*) gene, using 2-fluoroadenine (2-FA) resistance as a screen to select single or multiple gene knockout mutants.

In this study, we show that direct delivery of CRISPR-Cas9 RNPs can be used to induce targeted mutagenesis (TM) events in the brown alga *Ectocarpus* species 7. Initial experiments used a Droplet Digital™ PCR (ddPCR™) assay to detect TM events in populations of bombarded cells. Then CRISPR-Cas9 RNPs targeting the *Ectocarpus* species 7 *APT* gene were used to generate 2-FA-resistant (2-FAR) individuals bearing genetic mutations within the targeted regions of the *APT* locus. Two different CRISPR-Cas9 RNP introduction methods were used to generate 2-FAR individuals. Biolistic bombardment of *Ectocarpus* species 7 gametes produced 2-FAR partheno-sporophytes, whereas laser-assisted thermal-expansion microinjection of RNPs into developing unilocular sporangia generated 2-FAR gametophytes. Finally, we showed that simultaneous introduction of two different CRISPR-Cas9 RNPs, using either the biolistic or the microinjection approach, generated double gene knockouts, affecting both the selectable *APT* marker gene and one of three different additional, nonselected target genes. This study provides the first evidence of functional gene knockouts in a brown alga, opening a long-awaited era of reverse genetics for this key lineage. The availability of two different delivery strategies, biolistics and microinjection, allowing delivery of RNPs at different stages of the life cycle expands the scope of application of this new technology for the elucidation of brown algal gene function. Moreover, both of the targeted life cycle stages (partheno-sporophytes and gametophytes) are haploid, allowing direct observation of any phenotype associated with a mutated allele in first generation mutant individuals.

Materials and Methods

Guide RNA design and *in vitro* validation of ribonucleoprotein complexes

The CRISPOR (Concordet & Haeussler, 2018) tool (http://crispor.tefor.net/), with the *Ectocarpus* species 7 strain Ec32 genome as reference, was used to select the highest scoring crispr RNAs (crRNAs) for exons near the 5′ ends of target genes. Purified crRNAs, trans-activating crRNA (tracrRNA), and Cas9 protein (HiFi Cas9 Nuclease 3NLS) were obtained from Integrated DNA Technologies (IDT; Leuven, Belgium) and assembled into RNP complexes following the manufacturer's instructions with a Cas9 : gRNA ratio of 1 : 1. RNP *in vitro* cleavage assays were performed on purified PCR amplicons containing the target sites following the New England Biolabs online protocol (https://international.neb.com/protocols/2014/05/01/in-vitro-digestion-of-dna-with-cas9-nuclease-s-pyogenes-m0386). Briefly, 90 fmol of purified PCR amplicon was added to 900 fmol of preassembled RNP complex in NEBuffer 3.1 (New England Biolabs, Ipswich,

MA, USA) for a final volume of 30 µl. The reaction was incubated for 1 h at 37°C and the digestion was then terminated by addition of 1 µl Proteinase K (New England Biolabs) and incubation for 10 min at 65°C. The DNA digestion products were analysed on a 1.5% agarose gel. Supporting Information Table S1 provides the sequences of the crRNAs and oligonucleotide primer sequences used in this study.

Biological material

This study used the male *Ectocarpus* species 7 strain Ec32, for which a reference genome is available (Cock *et al.*, 2010; Cormier *et al.*, 2017). Strain Ec32 was previously referred to as *E. siliculosus* (Peters *et al.*, 2004), but a recent study (Montecinos *et al.*, 2017) indicates that it belongs to a distinct, at present unnamed, species, which is referred to provisionally as *Ectocarpus* species 7. *Ectocarpus* species 7 strain Ec32 was cultured in sterilized natural seawater enriched with half-strength Provasoli solution (Starr & Zeikus, 1993) (half-strength PES). The culture conditions were 13°C with a cycle of 12 h : 12 h, light : dark (20 µmol m^{-2} s^{-1}), and daylight-type fluorescent tubes (Coelho *et al.*, 2012) in the Roscoff laboratory and 15°C under cool white fluorescent lamps (30–40 µmol m^{-2} s^{-1}, 14 h : 10 h, light : dark) in the Muroran laboratory. All manipulations were performed under sterile conditions in a laminar flow hood.

Biolistic delivery of CRISPR-Cas9 ribonucleoprotein complexes

To obtain gametes for biolistic delivery, 2 mm gametophyte germlings were transferred to individual 140 mm Petri dishes (10 gametophytes per dish) containing 70 ml of culture medium. For each biolistic delivery, *c.* 100 fertile gametophytes bearing plurilocular gametangia were collected after 4 wk in culture and induced to release gametes (Coelho *et al.*, 2012) in 60 mm Petri dishes containing 5 ml of solidified (1.5% agar) culture medium by adding 10 ml of ice-cold sterile natural seawater. The gametophytes were removed after 6 h and the released gametes left to settle overnight on the agar substrate. Subsequent steps were performed using the same culture dishes, as settled gametes attach firmly to the agar substrate. The seawater medium was removed by delicate inversion 1 h before the experiment, and the agar plates were left to dry for 10 min under a laminar flow hood. Microparticle RNP coating and microcarrier preparation were performed as described by Serif *et al.* (2018). If not stated otherwise, 3 mg of gold (Au) nanoparticles (0.6 µm diameter; Bio-Rad) loaded with CRISPR-Cas9 RNPs, consisting of 8 µg Cas9 complexed with equimolar ratios of crRNA and tracrRNA, were used for each biolistic shot. Biolistic delivery parameters were a membrane rupture pressure of 1800 psi, a vacuum of 27 mmHg, and a target distance of 6 cm. Initial tests to verify delivery of nanoparticles to different cell types were carried out using 3 mg of Au nanoparticles (0.6 µm diameter; Bio-Rad) that had been preincubated in an 8 mM solution of AF488-labelled 10 kDa dextran (Invitrogen). Bombardments were carried out using a Bio-Rad PDS-1000/He system. After bombardment, 15 ml fresh culture medium was added and the gametes allowed to recover for 48 h prior to the application of selection by, for example, addition of 20 µM 2-FA (Sigma Aldrich). For ddPCR detection of TM events, biolistic delivery was performed on 2-wk-old immature gametophytes (five or six individuals per test) spread on the same solidified medium.

Laser-assisted thermal-expansion microinjection of CRISPR-Cas9 ribonucleoprotein complexes

Short branches bearing immature unilocular sporangia were dissected from sporophytes of *Ectocarpus* species 7 strain Ec32, placed on poly-L-lysine-coated coverslips, and immediately pushed gently with a cotton swab to ensure firm attachment. Two or three drops of half-strength PES medium were then added. The microinjection apparatus has been described previously (Nagasato *et al.*, 2015, 2017). Micromanipulators consisting of a coarse manipulator (MN-4; Narishige Co. Ltd, Tokyo, Japan) and a three-axis joystick oil hydraulic micromanipulator (MO-202; Narishige) were coupled to an Olympus IX71 inverted microscope (Olympus, Tokyo, Japan). Fine glass needles were produced by pulling glass capillaries (GDC-1; Narishige) with an MCF-100 microcapillary puller (Nepa Gene Co. Ltd, Tokyo, Japan). For the experiments that targeted only *APT*, a crRNA–tracrRNA mixture was prepared by mixing 1 µl of 100 µM gAPT1 crRNA, 1 µl of 100 µM tracrRNA, and 2 µl of microinjection buffer (20 mM HEPES, 150 mM potassium chloride, pH 7.0), heating to 95°C for 5 min, and then cooling to room temperature. The CRISPR-Cas9 RNP microinjection solution contained all 4 µl of the aforementioned crRNA–tracrRNA preparation plus 0.5 µl Cas9 (100 µg/10 µl; IDT) and 0.5 µl tetramethylrhodamine isothiocyanate conjugated 4.4 kDa dextran (Sigma; 10 mg ml^{-1} in water (H_2O)). The 5 µl CRISPR-Cas9 RNP microinjection solution was incubated for 5–10 min at room temperature and then dispensed into six microinjection needles. Silicone oil (ShinEtsu Co. Ltd, Tokyo, Japan), a laser absorbent (WF-25; Nepa Gene), and a UV absorbent (A-1428; Tesk Co. Ltd, Tokyo, Japan) were added to the glass needle. The CRISPR-Cas9 RNP solution was injected into unilocular sporangia using an LTM-1000 laser thermal microinjector (Nepa Gene).

A similar protocol was used for the experiments that simultaneously targeted *APT* and *MASTIGONEME1* (*MAS1*), except that two separate crRNA–tracrRNA mixtures were made by mixing 0.5 µl crRNA (either gAPT1 or Mas1-C), 0.5 µl tracrRNA, and 1.4 µl microinjection buffer, heating to 95°C and cooling, and then adding 0.4 µl Cas9. The two mixes were pooled and added to 0.4 µl rhodamine-conjugated 4.4 kDa dextran (10 mg ml^{-1} in H_2O). This solution was then treated as already described herein for microinjection. Stock solutions were as already described herein unless stated otherwise.

Droplet Digital PCR assays to detect CRISPR-Cas9-induced indel mutations

Indel detection was carried out using between four and 125 ng of total DNA on a QX200 ddPCR system with 5(6)-

carboxyfluorescein and hexachloro-fluorescein (HEX)-labelled oligonucleotide probes (Bio-Rad). Oligonucleotide primers and probes (Table S1) were obtained from Bio-Rad. ddPCR reactions were carried out by Ingénierie et Analyse en Genome Editing (Montferrier-sur-Lez, France), essentially as described previously (Mignerot *et al.*, 2019). A QX200 droplet generator (Bio-Rad) was used to distribute PCR components to individual reaction vessels. Droplets were generated by combining 70 µl of droplet generation oil with 22 µl of the PCR mix, and 40 µl of the resulting droplet reaction was subjected to amplification. The cycling conditions for the PCR reaction included an initial incubation for 10 min at 95°C followed by 40 cycles of 94°C for 30 s and 55°C for 60 s. Amplified plates were transferred to a droplet reader (Bio-Rad), and the digital PCR data were analysed with the provided QuantaSoft analytical software suite.

PCR detection of chromosomal mutations

Mutations at target genes, induced by the introduction of CRISPR-Cas9 RNPs, were detected by PCR amplification and Sanger sequencing. The PCR primers were the same as those used for the *in vitro* cleavage assays (Table S1).

Screen for off-target mutations

The genome of the 2-FAR mutant strain Ex1-1 was sequenced on an Illumina NovaSeq6000 platform (Génome Québec, Montreal, QC, Canada), generating 34.5 Gb of sequence data, corresponding to 114 273 283 2× 150 bp paired-end reads (SRA accession no. SRR12847952). The sequence reads were cleaned using Trimmomatic (Bolger *et al.*, 2014) (parameters: q 28, length 50, stringency 6, max_n 3, trimn) and mapped against the Ec32 reference genome (version v2, available at Orcae; Sterck *et al.*, 2012) using the Burrows–Wheeler aligner Bwa-Mem (Li, 2013). Variants were called using the HaplotypeCaller function of Gatk (McKenna *et al.*, 2010). Potential off-target sites were predicted using Crispor (Haeussler *et al.*, 2016) and searches for mutations at potential off-target sites were carried out using both the table of variants and by manual visualization of the genomic regions using the Integrative Genomics Viewer (Thorvaldsdóttir *et al.*, 2013).

In addition, the Ex1-1 resequencing data were used to carry out a genome-wide screen for variants that could potentially have arisen due to off-target activity. Because the *Ectocarpus* reference strain (Ec32) was sequenced in 2007 and has been maintained in culture since that time, filters were applied to exclude variants corresponding to either spontaneous mutations or sequencing errors. For this, we compared the Ex1-1 genome data, plus those of 19 other in-house sequenced mutant strains, with the *Ectocarpus* reference genome (strain Ec32). We then eliminated any variants that were detected in both Ex1-1 and at least one of the 19 other strains (i.e. corresponding to putative shared spontaneous mutations). Two variants were considered to be identical if they occurred within a window of 10 bp, because the variant detection pipeline did not always locate identical variants to exactly the same position in the genome (e.g. for small deletions or when the variant was located within a homopolymeric region). We also only considered positions with between 40× and 160× coverage and eliminated variants close to sequence gaps (runs of Ns). These latter filters were applied to eliminate sequence errors due to low coverage, aberrant mapping to repeated regions, or poor-quality sequence.

Results

Selection of target genes for mutagenesis

To facilitate the identification of mutant individuals, we focused on two genes that have been developed as positive selection systems in other algal species (Ferenczi *et al.*, 2017; Serif *et al.*, 2018). The two genes were *APT* (which, when mutated, has been shown to confer resistance to 2-FA; Fig. 1a) and *FK501-BINDING-PROTEIN 12* (*FKBP12*; which confers resistance to rapamycin when mutated). The *Ectocarpus* species 7 *APT* orthologue (LocusID Ec-28_000520) was identified by reciprocal blasts against the *Ectocarpus* species 7 reference genome (available via the ORCAE database; Sterck *et al.*, 2012; https://bioinformatics.psb.ugent.be/orcae/overview/EctsiV2), using both the *Physcomitrella patens* and the *Phaeodactylum tricornutum APT* genes as queries. Alignment of the three amino acid sequences confirmed conservation of the phosphoribosyl transferase domain in the *Ectocarpus* species 7 *APT* orthologue (Fig. 1b). A similar strategy (but employing orthologous sequences from *Chlamydomonas reinhardtii* and *Saccharomyces cerevisiae* as queries) was used to identify the *Ectocarpus* species 7 *FKBP12* gene (LocusID Ec-12_005100; Fig. 1c). crRNAs were designed to target the first and third exons of the *APT* gene (Fig. 1d) and the second exon of the *FKBP12* gene (Fig. 1e). CRISPR-Cas9 complexes carrying these crRNAs were shown to be active in an *in vitro* cleavage assay using PCR-amplified fragments of the targeted DNA regions (Fig. 1f).

Delivery of Cas9-ribonucleoproteins to *Ectocarpus* species 7 cells

Given the absence of a genetic transformation system for *Ectocarpus* species 7, the objective of this study was to develop a TM approach based on direct introduction of CRISPR-Cas9 RNPs. Two CRISPR-Cas9 RNP delivery methodologies were evaluated: biolistics and microinjection.

Gametes represent an interesting target material for biolistic delivery of CRISPR-Cas9 RNP complexes because they are single cells and they lack cell walls, facilitating entry of biolistic beads. In single-sex cultures of *Ectocarpus* species 7 gametophytes, released gametes develop parthenogenetically to produce haploid partheno-sporophytes (Fig. 2a). We observed that partheno-sporophyte germlings survived for several months on solidified, seawater-based medium (Fig. 2b), making this system suitable for the development of a biolistic delivery approach based on shooting gamete cells and subsequently recovering the derived partheno-sporophytes. Initial test experiments showed that biolistic delivery allowed AF488-labelled 10 kDa dextran to be loaded

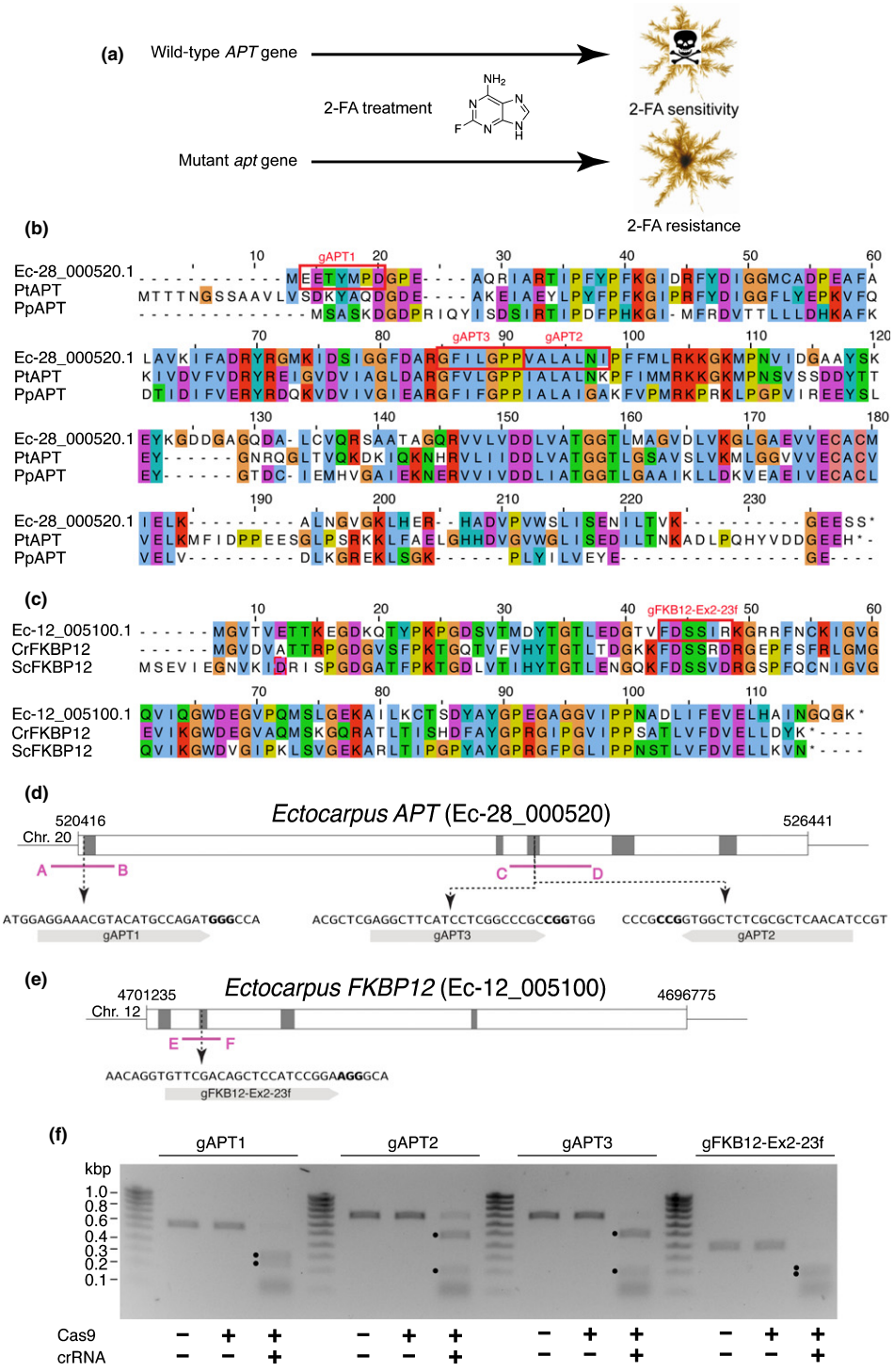

Fig. 1 Selection of target genes for CRISPR-Cas9-mediated mutagenesis and design of crispr RNAs (crRNAs). (a) Principle of the positive selection system using the *ADENINE PHOSPHORIBOSYL TRANSFERASE* (*APT*) marker gene, indicating the 2-fluoroadenine (2-FA) resistance phenotype of *apt* mutants. (b, c) Alignments of (b) APT and (c) FK501-BINDING-PROTEIN 12 (FKBP12) protein sequences. Conserved amino acids are highlighted in colour, and regions corresponding to crRNA target sites are indicated by red boxes. Pp, *Physcomitrella patens*; Pt, *Phaeodactylum tricornutum*; Cr, *Chlamydomonas reinhardtii*; Sc, *Saccharomyces cerevisiae*. (d, e) Schematic representations of the (d) *APT* and (e) *FKBP12* genes. Open boxes correspond to the transcribed regions of the genes and grey boxes to coding sequence. Light grey arrows indicate the positions of target sequences for crRNAs together with their associated protospacer adjacent motifs (in bold). Pink bars indicate the regions amplified to test the activity of CRISPR-Cas9 ribonucleoproteins (RNPs) *in vitro* or to detect mutations by Sanger sequencing. PCR primers (pink letters) were as follows: A, APT1-F-crispor; B, APT1-R2-500bp; C, APT2-F; D, APT1-R2-675bp; E, FKBex-F; F, FKBex2-R (see Supporting Information Table S1 for details). Chr. 20, chromosome 20; Chr. 12, chromosome 12. (f) *In vitro* activity tests of CRISPR-Cas9 RNPs directed against target regions in the *APT* and *FKBP12* genes. PCR amplicons containing the crRNA target sites were incubated with preassembled RNP complexes and the digestion products were then separated on a 1.5% agarose gel (see the Materials and Methods section for details). Black dots indicate digestion products. gAPT1, gAPT2, gAPT3 and gFKB12-Ex2-23f are different crRNAs directed against the *APT* or *FKBP12* genes.

into both gametophyte (Fig. 2c) and gamete cells (Fig. 2d), indicating the feasibility of delivering macromolecular complexes such as CRISPR-Cas9 RNPs using this approach.

For the microinjection approach, we targeted immature unilocular sporangia, because these structures contain a syncytium of multiple nuclei that will later become unispores, the

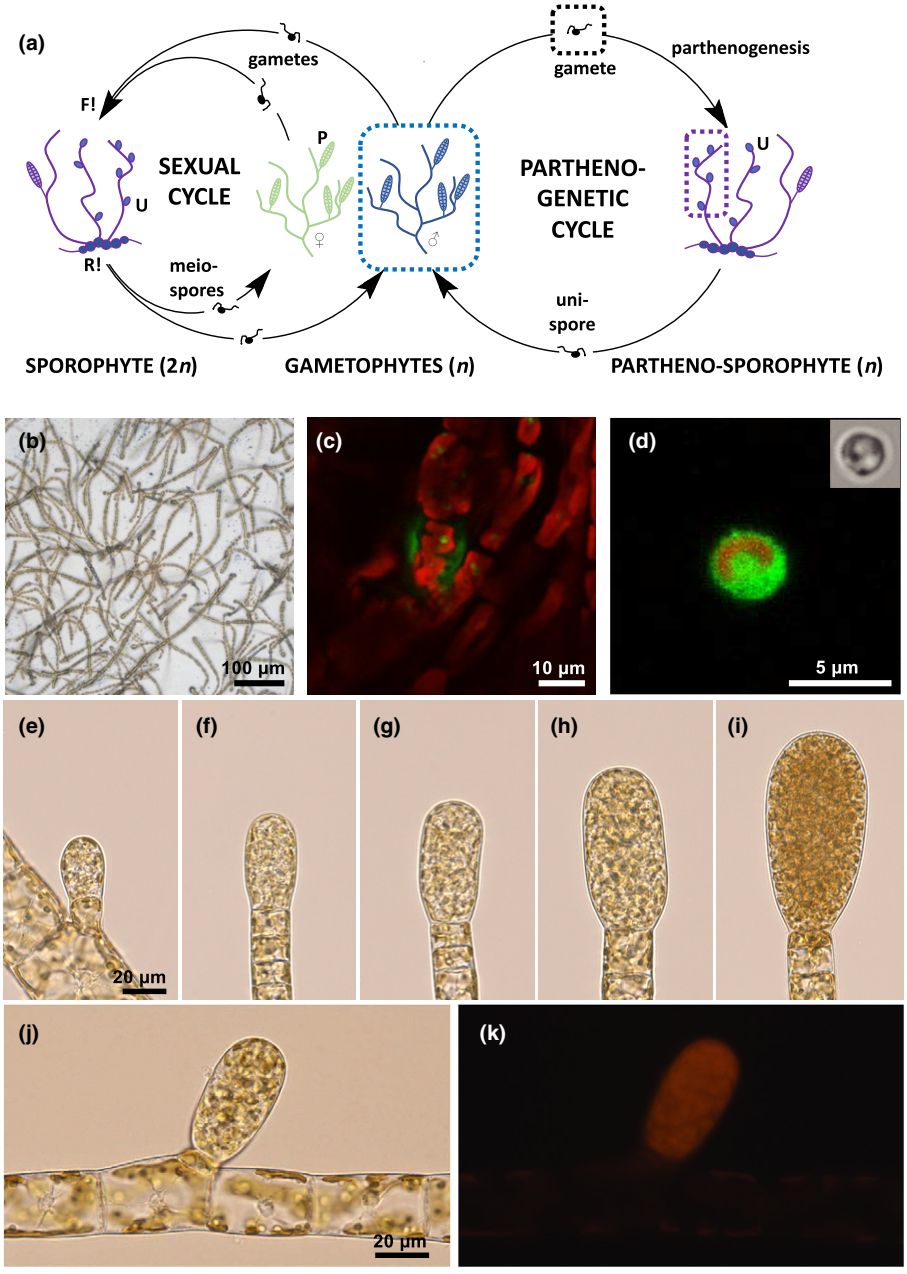

Fig. 2 Delivery of macromolecules into *Ectocarpus* species 7 cells by biolistics and microinjection. (a) Life cycle of *Ectocarpus* species 7. Meiosis (R!) occurs in unilocular sporangia (U) on the diploid sporophyte, producing meiospores that develop into male and female gametophytes. Gametophytes produce gametes in plurilocular gametangia (P), which fuse (F!) to produce the diploid sporophyte and complete the sexual cycle (left side of the panel). Gametes can also develop parthenogenetically to produce haploid partheno-sporophytes, which produce unilocular sporangia (U) that release spores to complete the parthenogenetic cycle (right side of the panel). We refer to the spores produced in the unilocular sporangia of partheno-sporophytes by the general term unispores because they are produced by nonstandard meiotic events (either apomeiosis or a meiosis-like division following endoreduplication; Bothwell *et al*., 2010). Dashed boxes indicate the life stages subjected to CRISPR-Cas9 ribonucleoprotein delivery for Droplet Digital™ PCR detection (blue, biolistic delivery to gametophytes) and gene knockout (black, biolistic delivery to gametes; purple, microinjection of unilocular sporangia). (b) *Ectocarpus* species 7 partheno-sporophytes growing on 1.5% seawater agar (1 month after gamete settlement). (c, d) Merges of Chl (red) and AF488-labelled 10 kDa dextran (green) fluorescence signals illustrating intracellular biolistic delivery of macromolecules into (c) gametophyte and (d) gamete cells. The inset in (d) is a transmitted-light image of the gamete. (e–i) Time series showing the development of a unilocular sporangium: (e) 8–16 nucleate stage; (f) 32 nucleate stage; (g) 64–128 nucleate stage; (h) 256 nucleate stage; (i) fully mature (512 nucleate) unilocular sporangium. Microinjection was carried out at stages (e)–(g). (j, k) Unilocular sporangium showing (red) fluorescence of microinjected rhodamine.

initial cells of the gametophyte generation (Fig. 2a). Laser-assisted thermal-expansion microinjection was used to deliver macromolecules to these structures because the cell wall and high turgor pressure of *Ectocarpus* species 7 cells make them hard to microinject with conventional techniques. As with the biolistic approach, fluorescently labelled markers were used to confirm that the microinjection approach allowed delivery of macromolecular complexes to immature unilocular sporangia (Fig. 2j, k).

Droplet Digital PCR detection of targeted mutagenesis events

As a first step to detect and quantitate TM events, we designed a drop-off ddPCR assay (Findlay *et al.*, 2016) based on mutation of *FKBP12* (Figs 1e, 3a). The biolistic approach was first tested on gametophytes, as we assumed that the larger size of their cells (20 µm compared with about 4 µm for gametes; Peters *et al.*, 2008; Lipinska *et al.*, 2015) would lead to higher rates of intracellular RNP delivery. Following biolistic delivery using various combinations of CRISPR-Cas9 RNP load, rupture pressure, and target distance, DNA was extracted from the entire target material for each biolistic shot and ddPCR was used to estimate the frequency of TM events. This approach detected a low but significant level of TM events in six out of a total of 14 experiments (Fig. 3b). These experiments indicated that CRISPR-Cas9 RNPs had been introduced into a subset of the *Ectocarpus* species 7 gametophyte cells by the biolistic delivery method and that they were active *in vivo*, inducing modifications at their target site in the *FKBP12* gene. ddPCR experiments were only carried out for mutations in the *FKBP12* gene and were not used to analyse mutations in the *APT* gene.

Isolation of mutant *Ectocarpus* species 7 individuals following biolistic delivery

The ddPCR experiments indicated that TM events were only induced in a small subset of the total population of cells targeted in the biolistic experiments. To isolate nonchimeric, mutant individuals, we therefore developed a positively selectable marker system and targeted a single cell stage: gametes. Wild-type gametes were allowed to develop parthenogenetically in the presence of either 10–20 µM 2-FA or 15 µM rapamycin to test the effectiveness of the two molecules as a selection system. These experiments showed that 10–20 µM 2-FA completely inhibited growth of wild-type *Ectocarpus* (Fig. S1). By contrast, growth of parthenogenetic gametes was not reliably inhibited in the presence of rapamycin, probably at least partially due to breakdown of the

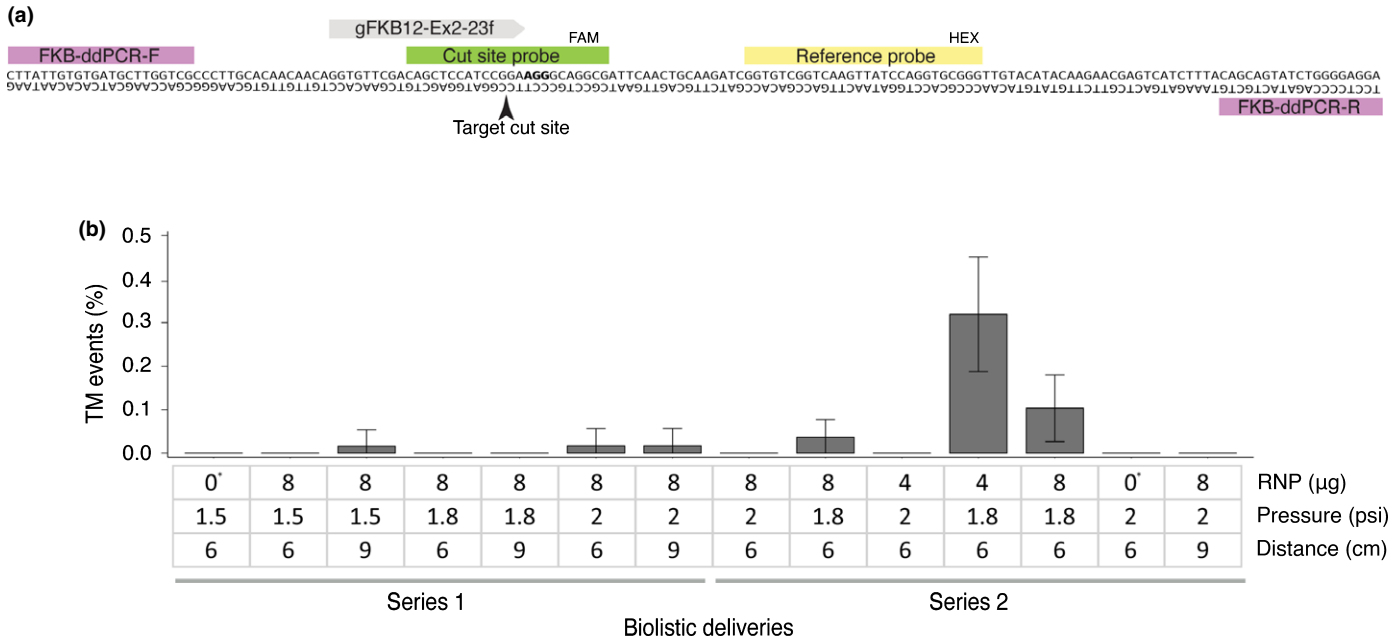

Fig. 3 Droplet Digital™ PCR (ddPCR™) detection of targeted mutagenesis events in gametophytes subjected to biolistic delivery of CRISPR-Cas9 ribonucleoproteins (RNPs). (a) Oligonucleotides employed for the drop-off ddPCR assay that was used to detect mutations in the second exon of the *FK501-BINDING-PROTEIN 12* (*FKBP12*) gene. The PCR primers (FKB-ddPCR-F and FKB-ddPCR-R, purple bars) and the reference probe (FKB-ddPCR-HEX, yellow bar) were designed distant from the site targeted by the CRISPR-Cas9 RNP complex, whereas the cut site probe (FKB-ddPCR-FAM, green bar) overlapped the site targeted by the crispr RNA (crRNA; gFKB12-Ex2-23f, grey arrow). The protospacer adjacent motif (PAM) is in bold. See Supporting Information Table S1 for details of the primers and crRNA. Fluorescent labels: FAM, 5(6)-carboxyfluorescein; HEX, hexachloro-fluorescein. (b) Frequencies of targeted mutagenesis events detected in 14 independent biolistic delivery experiments. Two series of biolistic experiments (series 1 and series 2) were carried out using gametes produced by two independently derived sets of gametophytes. Within each series, each Petri dish of target gametes was derived from a different gametophyte culture. Controls (*) were bombarded with Cas9 alone (8 µg). Frequencies of targeted mutagenesis events are expressed as ratios of single HEX (i.e. mutant) over double HEX + FAM (i.e. wild-type) fluorescent signals in droplets. Error bars correspond to the Poisson corrected fractional abundance calculated by the QuantaSoft software. TM, targeted mutagenesis.

antibiotic during culture. Based on these experiments, we decided to introduce CRISPR-Cas9 RNPs that targeted the *APT* gene. Biolistic experiments were then carried out using dense preparations of gametes (between *c.* 40 million and 60 million gametes per 60 mm plate) that had settled on an agar surface and CRISPR-Cas9 RNPs loaded with one of two crRNAs (either gAPT1 or gAPT2) targeting the first or the third exon of the *Ectocarpus* species 7 *APT* gene (Fig. 4a). Two days after bombardment, the culture medium was supplemented with 20 µM 2-FA and a small number of 2-FAR partheno-sporophytes developed in the Petri dishes after 4–6 wk in culture (see Fig. 4b for an experiment using gAPT1). Three out of eight gAPT1 and two out of three gAPT2 experiments yielded 2-FAR algae (Fig. 4a, and see the single crRNA experiments listed in Table S2). DNA was isolated from all of the 2-FAR individuals for high-fidelity PCR amplification, cloning, and sequencing of the *APT* locus. This revealed the occurrence of TM at the expected gAPT1 (Fig. 4c) and gAPT2 (Fig. 4d) CRISPR-Cas9 RNP cut sites, resulting in functional knockouts of the *Ectocarpus* species 7 *APT* gene. All the 2-FAR individuals from the gAPT1 experiments had an additional adenine residue inserted between positions 520 479 and 520 480, three nucleotides before the protospacer adjacent motif (PAM), inducing a frame shift in the coding sequence of the *APT* gene. The 2-FAR individuals from the gAPT2 experiments had deletions of one or four nucleotides three nucleotides before the PAM, which also resulted in frame shifts.

Isolation of mutant *Ectocarpus* species 7 individuals following microinjection of unilocular sporangia

We next determined whether it was possible to isolate individuals with TM events in the *APT* gene following laser-assisted thermal-

(a)

crRNA	Total shots	2-FAR individuals	Validated TMs	Successful shots
gAPT1	8	8	3	3
gAPT2	3	5	3	2

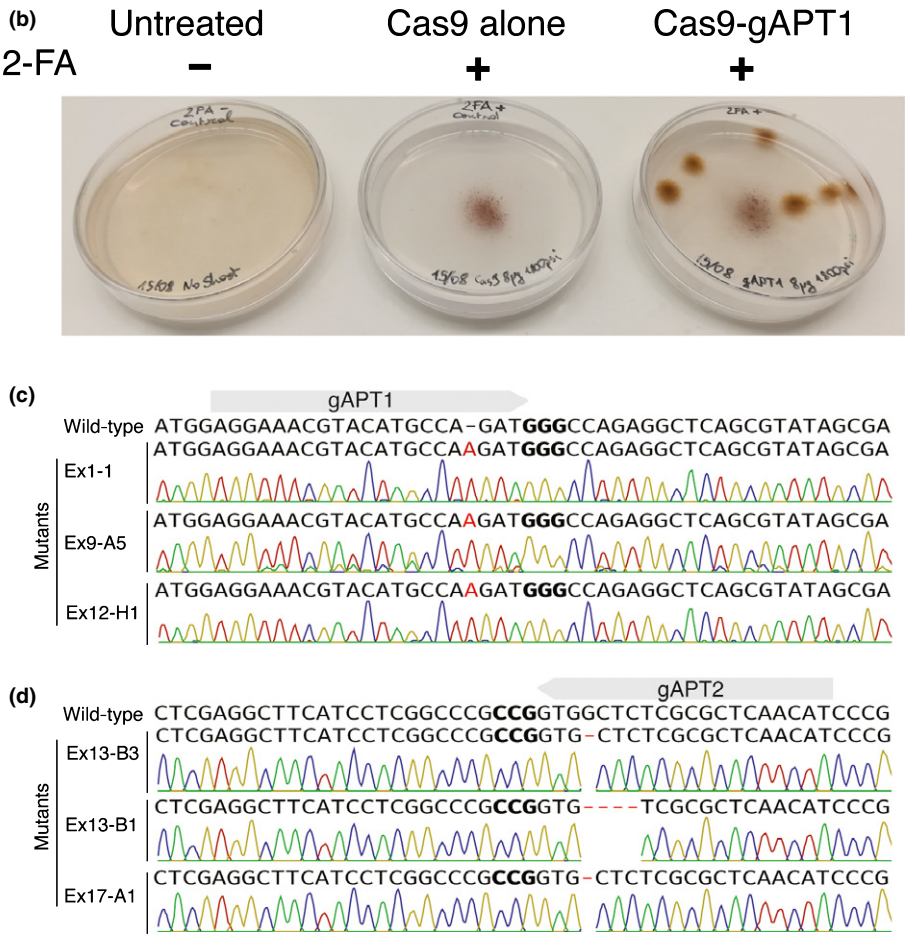

Fig. 4 Isolation of individuals with mutations in the *ADENINE PHOSPHORIBOSYL TRANSFERASE* (*APT*) gene following biolistic delivery of CRISPR-Cas9 ribonucleoproteins (RNPs). (a) Number of 2-fluoroadenine (2-FA)-resistant (2-FAR) individuals and confirmed targeted mutagenesis (TM) events obtained in 11 experiments using either the gAPT1 or gAPT2 crispr RNA (crRNA). Validated TM indicates the number of 2-FAR individuals in which a TM event was detected by Sanger sequencing. 'Successful shot' indicates the number of experiments where at least one TM event was detected. (b) Biolistic experiment showing five 2-FAR individuals obtained after biolistic delivery of gAPT1 RNPs (the more diffuse brown mark in the centre of the Petri dish corresponds to the bombarded gold beads). The three Petri dishes correspond to untreated gametes (left) or to gametes exposed to 2-FA following bombardment either with 8 µg Cas9 with no crRNA (middle) or with 8 µg of gAPT1 RNPs (right). Note that the Petri dishes were photographed 3 months postbombardment, when the 2-FAR individuals were clearly visible, but 2-FAR candidates can be detected using a stereomicroscope as early as 3–4 wk postbombardment. (c, d) Sanger sequence chromatograms for the six 2-FAR individuals obtained using (c) gAPT1 or (d) gAPT2 crRNAs. Protospacer adjacent motifs are in bold.

expansion microinjection of unilocular sporangia with gAPT1 CRISPR-Cas9 RNP. Two unilocular sporangia were injected with gAPT1 CRISPR-Cas9 RNP at the 8–32 nucleate stage (Fig. 5a). The unilocular sporangia developed to maturity and released their unispores 5 d after microinjection. Four days after unispore release, 2-FA was added to the half-strength PES seawater medium to a final concentration of 20 µM. After a further 7 d, 11 of the 2-FAR individuals were detected and isolated. These individuals were transferred to fresh medium containing 20 µM 2-FA in multiwell plates along with wild-type gametophytes as a control (Fig. 5b). PCR amplification and Sanger sequencing of the region of exon 1 of the *APT* gene targeted by the gAPT1 CRISPR-Cas9 RNP showed that all 11 individuals carried the same mutation, an inserted adenine residue between nucleotides 520 479 and 520 480, at the site targeted by gAPT1 (Fig. 5c,d; Table S2). Following meiotic division of the mother cell in a developing unilocular sporangium, the four daughter cells undergo several mitotic divisions to produce at least 100 meiospores per unilocular sporangium (Knight, 1929; Peters *et al.*, 2008). This phenomenon has been reported in diploid sporophytes, but a similar process occurs in the unilocular sporangia of partheno-sporophytes. It is possible, therefore, that some of the mutant individuals were clonally derived from the same TM event but at least two mutation events must have occurred (one in each unilocular sporangium). Note also that the inserted adenine residue was the same mutation as had been previously detected following biolistic delivery of gAPT1 CRISPR-Cas9 RNP (Fig. 3c). This experiment demonstrated that CRISPR-Cas9 RNPs enter the nuclei of developing unispores following microinjection into unilocular sporangia, where they efficiently induce targeted mutation of the algal genome. The absence of false-positive 2-FAR individuals indicated that 2-FA treatment selected mutant individuals more efficiently in the microinjection experiments than in the biolistic experiments, possibly because the selection system is more effective when applied to a small number of individuals (up to *c.* 500 for the microinjection experiments compared with many thousands for the biolistic experiments).

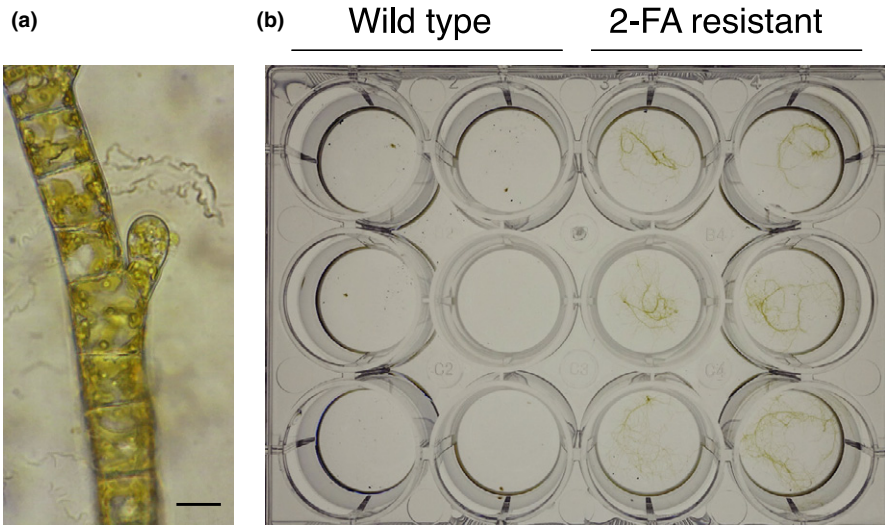

(c)

Unilocular sporangium	crRNA	N° of 2-FAR individuals with *apt* mutation
1	gAPT1	7
2	gAPT1	4

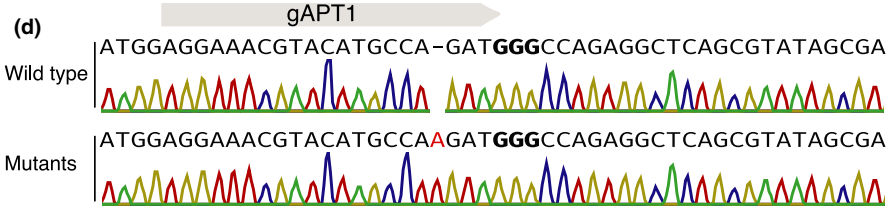

Fig. 5 Isolation of 2-fluoroadenine (2-FA)-resistant (2-FAR) gametophytes after microinjection of unilocular sporangia. (a) An 8–16 nucleate stage unilocular sporangium after microinjection. Bar, 20 µm. (b) Wild-type and 2-FAR gametophytes that were cultured in a multiwell plate in half strength Provasoli solution containing 20 µM 2-FA for 9 d at 15°C with long-day illumination. The 2-FAR gametophytes correspond to six of the seven individuals derived from the first unilocular sporangia microinjected with the gAPT1 CRISPR-Cas9 ribonucleoprotein targeting the *APT* gene. (c) Summary of the 2-FAR individuals isolated following microinjection of each of the two unilocular sporangia. (d) Location of the single inserted adenine residue (in red) detected at the target site in all 11 of the 2-FAR individuals isolated following microinjection. The region corresponding to the gAPT1 crRNA is indicated by a grey arrow, and the protospacer adjacent motif is shown in bold. A representative chromatogram is shown for the mutant individuals.

Simultaneous creation of double mutants potentially allows the mutation of any targeted locus

The aforementioned experiments demonstrated that it is possible to isolate individuals with targeted mutations provided that a positive selection system is available for the induced mutants. However, to develop an effective reverse genetic methodology, it was necessary to extend this approach so that it could be applied to any selected target gene. For this, we determined whether it was possible to isolated double mutants affected simultaneously at a positively selectable locus and at a second, target gene. Biolistic delivery was used to introduce mixtures of CRISPR-Cas9 RNPs carrying two different crRNAs, either targeting two different regions of the *APT* gene or simultaneously targeting *APT* plus a second gene (which was *FKBP12* for these test experiments). Eleven biolistic shots were carried out using different combinations of pairs of crRNAs (Fig. 6; Table S2). These experiments allowed the isolation of 17 2-FAR individuals, including two individuals that were mutated at two independent sites. The first individual carried a double mutation in the *APT* gene, corresponding to the sites targeted by gAPT2 and gAPT3, whereas the second individual carried mutations at the targeted sites in both the *APT* and the *FKBP12* gene (Fig. 6). In both cases, the mutant individuals were isolated solely based on their resistance to 2-FA. Analysis of the *apt fkbp12* double mutant in culture showed that the morphology of the partheno-sporophyte generation was normal and that the strain was fully fertile, producing both plurilocular and unilocular sporangia (Fig. S2). Moreover, gametophytes derived from unispores produced by the *apt fkbp12* partheno-sporophyte were also morphologically normal and fertile, producing plurilocular gametangia (Fig. S2). Therefore, mutation of the *APT* gene did not appear to have any phenotypic effect on either development or reproduction. This experiment demonstrated the feasibility of applying the methodology to any target gene in the *Ectocarpus* genome (with the proviso that the mutation should not be lethal, at least when haploid strains are being mutagenized).

To further validate the methodology, CRISPR-Cas9 RNPs carrying crRNAs directed against *APT* (gAPT1) and a second target gene *VANADIUM-DEPENDENT BROMOPEROXIDASE* (*VBPO*, locusID Ec-28_003320; crRNA vBPO-ex6-228f) were simultaneously delivered into gamete cells using the biolistic methodology. Two 2-FAR individuals were isolated from five experiments. One of these individuals was mutated at both the *APT* target site and the target site in the *VBPO* gene (Fig. 6; Table S2). These experiments demonstrated that double mutants could be reproducibly obtained using biolistic delivery.

To demonstrate that double mutants could also be obtained using the microinjection approach, 25 unilocular sporangia were injected with a mixture of CRISPR-Cas9 RNPs carrying gAPT1 and a crRNA (Mas1-C) directed against the *MAST1* gene (Ec-04_001260), which is predicted to encode a mastigoneme protein. Thirteen of these unilocular sporangia released their unispores. Growth of these unispores on 2-FA resulted in the isolation of 22 2-FAR mutants from five different unilocular sporangia. PCR amplification and sequencing of the target sites of the *APT* and *MAS1* genes in 13 of these mutants identified nine individuals that carried mutations in both genes (Fig. 6; Table S2). Note, however, that all 13 of the 2-FAR individuals were derived from the same injected unilocular sporangium, so we cannot rule out the possibility that some of the mutant individuals were clonally derived from the same TM event.

Efficiency of CRISPR-Cas9-mediated gene mutation

The results of all of the experiments described in the two previous sections (Table S2) were analysed to estimate how efficiently the two methodologies, biolistics and microinjection, generated mutant individuals. Analysis of the experiments in which a single type of CRISPR-Cas9 RNP was introduced into *Ectocarpus* cells indicated that 33.3% and 18.2% of biolistic and microinjection experiments (where an experiment is either one biolistic shot or one injected unilocular sporangium), respectively, resulted in the isolation at least one *apt* mutant (Table S2). The percentages of 2-FAR individuals that carried a mutation in the *APT* gene in these experiments was 46.2% and 100%, for the biolistic and microinjection approaches, respectively. The average number of *apt* mutants obtained per experiment was 0.4 and 1.0 for the biolistic and microinjection methodologies, respectively.

For the biolistic experiments that involved simultaneous introduction of two different CRISPR-Cas9 RNPs, we detected *apt* mutants in 50.0% (eight out of 16) of the experiments. Of the 14 *apt* mutants identified, 21.4% (three individuals) were double knockouts. Double knockouts were detected in 18.8% of the experiments (Table S2). For the microinjection experiments that involved simultaneous introduction of two different CRISPR-Cas9 RNPs, we detected 2-FAR individuals in 20.0% of the experiments (five out of 25 experiments, but note that 12 of the 20 unilocular sporangia that did not produce 2-FAR individuals did not release their unispores and, therefore, it was not possible to apply 2-FA selection). A total of 22 of the 2-FAR individuals were isolated from the 25 experiments (0.9 per experiment on average). Sequence analysis of 13 of the 2-FAR individuals isolated from one of these experiments demonstrated that 31% (four individuals) were only mutated at the *APT* locus, whereas 69% (nine individuals) carried mutations at both the *APT* and *MAS1* loci (Table S2).

Off-target mutations

To estimate the frequency of off-target mutations, the genome of one of the *apt* mutants (Ex1-1; Fig. 4) was resequenced using an Illumina platform and the sequence data were analysed for evidence of mutations at potential off-target sites for the crRNA gAPT1 predicted by Crispor (Haeussler *et al.*, 2016). No mutations were detected at any of the five potential off-target sites (Table S3), indicating that the approach used does not induce a high frequency of off-target mutations.

In addition, we carried out a genome-wide analysis of variants in the genome of the Ex1-1 mutant (see the Materials and Methods section for details). This analysis detected 56 variants

(a)

crRNAs	Total shots or injections	Number of 2-FAR individuals	Single TM (%)	Double TM (%)
gAPT1 + gAPT2	1	8	50	0
gAPT2 + gAPT3	1	1	0	100*
gAPT1 + gFKB12	9	8	75	13
gAPT1 + vBPO-ex6-228f	5	2	50	50
gAPT1 + Mas1-C	25	22	31**	69**

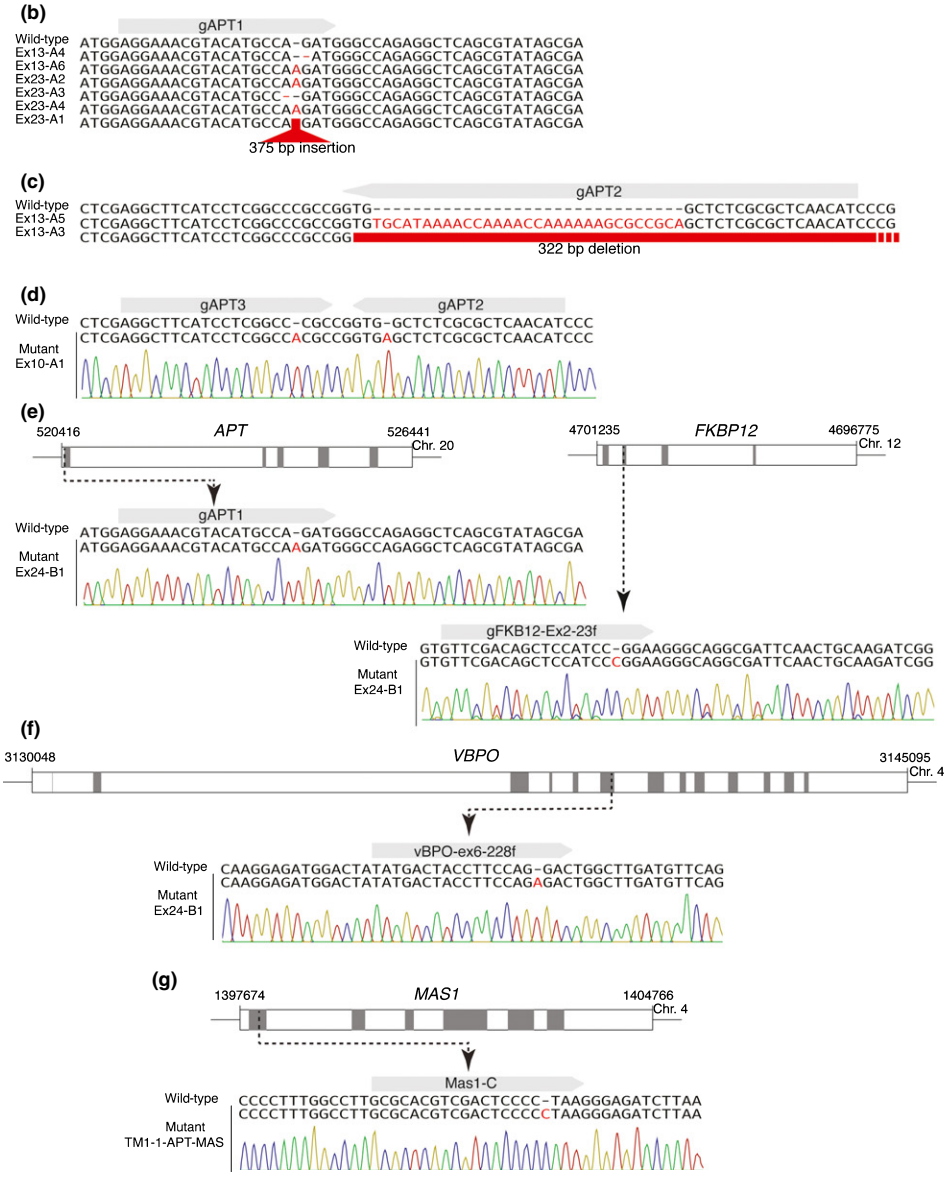

Fig. 6 Simultaneous recovery of mutations in a selectable gene and in a second, target gene. (a) Percentages of confirmed single and double targeted mutagenesis (TM) events observed in 41 experiments that used combinations of two different CRISPR-Cas9 ribonucleoproteins (RNPs.) *, In this case the two mutations were in two different regions of the *ADENINE PHOSPHORIBOSYL TRANSFERASE* (*APT*) gene. **, Estimations based on sequencing of 13 of the 22 2-fluoroadenine-resistant individuals. (b, c) Diversity of single TM events obtained at the (b) gAPT1 and (c) gAPT2 target sites. (d) Detection of a double TM event at the *APT* locus. (e) Detection of a double TM event resulting in the knockout of both the *Ectocarpus* species 7 *APT* and *FK501-BINDING-PROTEIN 12* (*FKBP12*) genes after biolistic introduction of a mixture of CRISPR-Cas9 RNPs targeting the two genes. (f) Detection of a mutation in the *VANADIUM-DEPENDENT BROMOPEROXIDASE* (*VBPO*) gene after simultaneous biolistic introduction of a mixture of two CRISPR-Cas9 RNPs targeting *APT* and *VBPO*. (g) Detection of a mutation in the *MASTIGONEME1* (*MAS1*) gene after simultaneous microinjection of a mixture of two CRISPR-Cas9 RNPs targeting *APT* and *MAS1*. Only the mutations in the *VBPO* and *MAS1* genes are shown, and only one representative chromatogram is shown for the *mas1* mutants. For the gene drawings, open boxes correspond to the transcribed regions of the genes, and grey boxes to coding sequence. Transcription is from left to right. Chr. 20, chromosome 20; Chr. 12, chromosome 12; Chr. 4, chromosome 4.

compared with the *Ectocarpus* reference genome (Table S4). Many of these variants were located in microsatellites, consistent with them corresponding to spontaneous mutations. Alignment of the variant regions with the gAPT1 crRNA indicated that none of them were in sequence contexts that would have been consistent with off-target effects of the CRISPR-Cas9 RNP (Table S4). Conversely, 243 regions with weak similarity to gAPT1 (plus its PAM sequence) were detected by a very low stringency BLAST search against the genome, and none of these matching sequences were located within 400 bp of a sequence variant. These analyses, therefore, supported our conclusion that off-target mutations were extremely rare or absent.

Discussion

This study has demonstrated the feasibility of using direct introduction of CRISPR-Cas9 RNPs into brown algal cells to induce targeted mutations. In particular, with the demonstration that induced, targeted mutations in the *APT* gene can be used to select for individuals carrying a mutation at a second targeted locus, it is now theoretically possible to mutate any selected gene in the *Ectocarpus* genome. One limiting factor may be lethality associated with mutation of essential genes, given that both of the delivery methods described here use haploid target cells. However, even for these genes, it may be possible to recover non-null mutations that nonetheless exhibit informative phenotypes. Moreover, in the future it should be feasible to build on the methodologies described here to develop a protocol that employs diploid cells, such as the mitospores produced by diploid sporophytes for example.

As far as the efficiency of the two methods presented here is concerned, 2-FAR individuals were obtained in 52% and 19% of biolistic and microinjection experiments, respectively, and, on average, we obtained 1.2 and 0.9 2-FAR individuals per experiment, respectively. The limited number of experiments did not allow us to obtain a precise measurement of the percentage of double knockout mutants, but this was estimated at 18% and 69% of the *apt* mutants isolated after introduction of two different CRISPR-Cas9 RNPs by either biolistics or microinjection, respectively. The methodology presented here, therefore, is sufficiently efficient and reproducible for it to be used reliably to isolate mutations for any selected *Ectocarpus* gene.

There are several advantages to directly introducing CRISPR-Cas9 RNPs into target cells rather than using an *in vivo* expression system. First, it is not necessary that a transformation protocol be available for the target species. Second, the methodology is relatively easy to employ because it does not require the construction of complex transformation vectors. Third, following direct introduction, the CRISPR-Cas9 RNPs are only present transiently in the cell, and therefore the frequency of off-target mutations is expected to be lower than if CRISPR-Cas9 RNPs are expressed over an extended period (Kim *et al.*, 2014). This expectation was supported by the absence of mutations at potential off-target sites in the *apt* mutant Ex1-1. Finally, as pointed out by Serif *et al.* (2018), the aforementioned advantages, in particular the absence of a need for genetic transformation, mean that it should be relatively easy to adapt such methodology for use in related species. Specifically, it should be possible to adapt the methodology described here for other brown algal species, provided that a suitable protocol is available to deliver CRISPR-Cas9 RNPs into cells and that the *APT*-based selection system used is effective in the new species. It may even be possible to circumvent the need for a selection system if microinjection can be used to deliver CRISPR-Cas9 RNPs to well-identified cells that can be isolated postinjection.

The availability of an effective reverse genetics tool for *Ectocarpus* opens up multiple avenues for both fundamental and applied brown algal research. In the fundamental domain, this tool will allow the brown algal community to investigate the functions of multiple genes implicated in diverse aspects of brown algal biology, particularly those associated with novel features or features of broad phylogenetic interest, such as the emergence of complex multicellularity, the evolution of complex, highly flexible cell walls, haploid-phase sex determination, and novel metabolic processes or interactions with both biotic and abiotic factors (Michel *et al.*, 2010a; Ahmed *et al.*, 2014; Cock *et al.*, 2014; Cock & Collén, 2015; Dittami *et al.*, 2016; Strittmatter *et al.*, 2016; Coelho & Cock, 2020). From a more applied point of view, the availability of reverse genetics will greatly enhance the usefulness of *Ectocarpus* as a model organism to understand brown algal traits that are relevant to seaweed aquaculture, such as genetic factors underlying growth and biomass production (Avia *et al.*, 2017), metabolic pathways influencing biomolecule content (La Barre *et al.*, 2010; Michel *et al.*, 2010a,b), and the defence mechanisms that control and prevent disease (Gachon *et al.*, 2010). In addition, the ability to target specific genes may potentially make *Ectocarpus* itself interesting for biotechnological applications; for example, using the organism as a cell factory. In this context, the availability of mutant strains that have lost the ability to adhere to substrata (Godfroy *et al.*, 2017) may be of interest for the cultivation of this species in bioreactors.

Finally, in addition to adapting the existing CRISPR-Cas9-based system to other brown algae, another important objective for the future will be to extend and improve the CRISPR-Cas9-based tools available for *Ectocarpus*. For example, the targeted mutations reported here presumably result from the action of the nonhomologous end joining repair pathway. The involvement of this pathway could be exploited to develop gene knock-in strategies using simultaneous delivery of donor DNA (Suzuki *et al.*, 2016). Likewise, it will be interesting to test the effectiveness of alternatives to the Cas9 nuclease (Zetsche *et al.*, 2015; Pausch *et al.*, 2020) and, in the longer term, to adapt more sophisticated methodologies, such as homology-mediated gene editing (Savić *et al.*, 2019) or prime editing (Anzalone *et al.*, 2019), for use in this key model organism.

Acknowledgements

We would like to thank Anne De Cian and Fayza Daboussi for advice on the CRISPR system and for supplying Cas9 proteins, and Dominique Marie for help with flow cytometry analysis of *Ectocarpus* gametes. This work was supported by the Région Bretagne's Stratégie d'Attractivité Durable (SAD) program (grant to

support YB), the Marine Alliance for Science and Technology Scotland, a UK Natural Environment Research Council International Opportunities Fund Pump-priming Award (NE/L013223/1), the European Research Council (SexSea grant agreement 638240), the European Union's Horizon 2020 research and innovation programme ASSEMBLE Plus project (grant agreement no. 730984), the Agence Nationale de la Recherche projects Epicycle and Idealg (ANR-19-CE20-0028-01 and ANR-10-BTBR-04-01), the Centre National de la Recherche Scientifique, the Gordon and Betty Moore Foundation program Symbiosis in Aquatic Systems Initiative (grant agreement 4546891618), Sorbonne University, and the European Union COST program Phycomorph. We thank the Institut Français de Bioinformatique and the Roscoff Analysis and Bioinformatics for Marine Science platform ABiMS (http://abims.sb-roscoff.fr) for providing computing and data storage resources.

Author contributions

YB conceived the project and carried out the biolistic experiments with help from DS and MR. MH, TM, and CN developed the microinjection approach and carried out the microinjection experiments. CC and DS explored and optimized delivery methodologies. OG and YB carried out the variant analysis. TM, CN, CMMG, SMC, and JMC supervised the project. YB and JMC wrote the manuscript with input from all the authors.

ORCID

Yacine Badis https://orcid.org/0000-0003-1606-3906
J. Mark Cock https://orcid.org/0000-0002-2650-0383
Susana M. Coelho https://orcid.org/0000-0002-9171-2550
Claire M. M. Gachon https://orcid.org/0000-0002-3702-7472
Olivier Godfroy https://orcid.org/0000-0002-8963-8371
Delphine Scornet https://orcid.org/0000-0002-1895-8909

References

Ahmed S, Cock J, Pessia E, Luthringer R, Cormier A, Robuchon M, Sterck L, Peters A, Dittami S, Corre E *et al.* 2014. A haploid system of sex determination in the brown alga *Ectocarpus* sp. *Current Biology* **24**: 1945–1957.

Anzalone AV, Randolph PB, Davis JR, Sousa AA, Koblan LW, Levy JM, Chen PJ, Wilson C, Newby GA, Raguram A *et al.* 2019. Search-and-replace genome editing without double-strand breaks or donor DNA. *Nature* **576**: 149–157.

Arun A, Coelho SM, Peters AF, Bourdareau S, Pérès L, Scornet D, Strittmatter M, Lipinska AP, Yao H, Godfroy O *et al.* 2019. Convergent recruitment of TALE homeodomain life cycle regulators to direct sporophyte development in land plants and brown algae. *eLife* **8**: e43101.

Avia K, Coelho SM, Montecinos AE, Cormier A, Lerck F, Mauger S, Faugeron S, Valero M, Cock JM, Boudry P. 2017. High-density genetic map and identification of QTLs for responses to high temperature and low salinity stresses in the model alga *Ectocarpus* sp. *Scientific Reports* **7**: e43241.

Bolger AM, Lohse M, Usadel B. 2014. Trimmomatic: a flexible trimmer for Illumina sequence data. *Bioinformatics* **30**: 2114–2120.

Bothwell JH, Marie D, Peters AF, Cock JM, Coelho SM. 2010. Role of endoreduplication and apomeiosis during parthenogenetic reproduction in the model brown alga *Ectocarpus*. *New Phytologist* **188**: 111–121.

Bourdareau S, Tirichine L, Lombard B, Loew D, Scornet D, Wu Y, Coelho SM, Cock JM. 2021. Histone modifications during the life cycle of the brown alga *Ectocarpus*. *Genome Biology* **22**: e12.

Cho SW, Lee J, Carroll D, Kim J-S, Lee J. 2013. Heritable gene knockout in *Caenorhabditis elegans* by direct injection of Cas9-sgRNA ribonucleoproteins. *Genetics* **195**: 1177–1180.

Chung IK, Beardall J, Mehta S, Sahoo D, Stojkovic S. 2011. Using marine macroalgae for carbon sequestration: a critical appraisal. *Journal of Applied Phycology* **23**: 877–886.

Cock JM, Collén J. 2015. Independent emergence of complex multicellularity in the brown and red algae. In: Ruiz-Trillo I, Nedelcu AM, eds. *Advances in marine genomics. Evolutionary transitions to multicellular life*. Dordrecht, the Netherlands: Springer Verlag, 335–361.

Cock JM, Godfroy O, Macaisne N, Peters AF, Coelho SM. 2014. Evolution and regulation of complex life cycles: a brown algal perspective. *Current Opinion in Plant Biology* **17**: 1–6.

Cock JM, Sterck L, Rouzé P, Scornet D, Allen AE, Amoutzias G, Anthouard V, Artiguenave F, Aury J-M, Badger JH *et al.* 2010. The *Ectocarpus* genome and the independent evolution of multicellularity in brown algae. *Nature* **465**: 617–621.

Coelho S, Cock J. 2020. Brown algal model organisms. *Annual Review of Genetics* **54**: 71–92.

Coelho SM, Scornet D, Rousvoal S, Peters NT, Dartevelle L, Peters AF, Cock JM. 2012. How to cultivate *Ectocarpus*. *Cold Spring Harbor Protocols* **2012**: 258–261.

Coleman MA, Goold HD. 2019. Harnessing synthetic biology for kelp forest conservation. *Journal of Phycology* **55**: 745–751.

Coleman MA, Wernberg T. 2017. Forgotten underwater forests: the key role of fucoids on Australian temperate reefs. *Ecology and Evolution* **7**: 8406–8418.

Concordet J-P, Haeussler M. 2018. Crispor: intuitive guide selection for CRISPR/Cas9 genome editing experiments and screens. *Nucleic Acids Research* **46**: W242–W245.

Cormier A, Avia K, Sterck L, Derrien T, Wucher V, Andres G, Monsoor M, Godfroy O, Lipinska A, Perrineau M-M *et al.* 2017. Re-annotation, improved large-scale assembly and establishment of a catalogue of noncoding loci for the genome of the model brown alga *Ectocarpus*. *New Phytologist* **214**: 219–232.

Dittami SM, Duboscq-Bidot L, Perennou M, Gobet A, Corre E, Boyen C, Tonon T. 2016. Host–microbe interactions as a driver of acclimation to salinity gradients in brown algal cultures. *ISME Journal* **10**: 51–63.

Dittami SM, Scornet D, Petit J-L, Ségurens B, Da Silva C, Corre E, Dondrup M, Glatting K-H, König R, Sterck L *et al.* 2009. Global expression analysis of the brown alga *Ectocarpus siliculosus* (Phaeophyceae) reveals large-scale reprogramming of the transcriptome in response to abiotic stress. *Genome Biology* **10**: R66.

Duarte CM, Wu J, Xiao X, Bruhn A, Krause-Jensen D. 2017. Can seaweed farming play a role in climate change mitigation and adaptation? *Frontiers in Marine Science* **4**: e100.

Fang Y, Cui L, Gu B, Arredondo F, Tyler BM. 2017. Efficient genome editing in the oomycete *Phytophthora sojae* using CRISPR/Cas9. *Current Protocols in Microbiology* **44**: 21A.1.1–21A.1.26.

Farnham G, Strittmatter M, Coelho SM, Cock JM, Brownlee C. 2013. Gene silencing in *Fucus* embryos: developmental consequences of RNAi-mediated cytoskeletal disruption. *Journal of Phycology* **49**: 819–829.

Ferenczi A, Pyott DE, Xipnitou A, Molnar A. 2017. Efficient targeted DNA editing and replacement in *Chlamydomonas reinhardtii* using *Cpf*1 ribonucleoproteins and single-stranded DNA. *Proceedings of the National Academy of Sciences, USA* **114**: 13567–13572.

Findlay SD, Vincent KM, Berman JR, Postovit L-M. 2016. A digital PCR-based method for efficient and highly specific screening of genome edited cells. *PLoS ONE* **11**: e0153901.

Gachon CM, Sime-Ngando T, Strittmatter M, Chambouvet A, Kim GH. 2010. Algal diseases: spotlight on a black box. *Trends in Plant Science* **15**: 633–640.

Godfroy O, Uji T, Nagasato C, Lipinska AP, Scornet D, Peters AF, Avia K, Colin S, Mignerot L, Motomura T *et al.* 2017. DISTAG/TBCCd1 is required for basal cell fate determination in *Ectocarpus*. *Plant Cell* **29**: 3102–3122.

Gschloessl B, Guermeur Y, Cock J. 2008. HECTAR: a method to predict subcellular targeting in heterokonts. *BMC Bioinformatics* **9**: e393.

Haeussler M, Schönig K, Eckert H, Eschstruth A, Mianné J, Renaud J-B, Schneider-Maunoury S, Shkumatava A, Teboul L, Kent J *et al.* 2016. Evaluation of off-target and on-target scoring algorithms and integration into the guide RNA selection tool CRISPOR. *Genome Biology* **17**: e148.

Heesch S, Cho GY, Peters AF, Le Corguillé G, Falentin C, Boutet G, Coëdel S, Jubin C, Samson G, Corre E *et al.* 2010. A sequence-tagged genetic map for the brown alga *Ectocarpus siliculosus* provides large-scale assembly of the genome sequence. *New Phytologist* **188**: 42–51.

Hirata R, Takahashi M, Saga N, Mikami K. 2011. Transient gene expression system established in *Porphyra yezoensis* is widely applicable in Bangiophycean algae. *Marine Biotechnology* **13**: 1038–1047.

Jiang P, Qin S, Tseng CK. 2003. Expression of the *lacZ* reporter gene in sporophytes of the seaweed *Laminaria japonica* (Phaeophyceae) by gametophyte-targeted transformation. *Plant Cell Reports* **21**: 1211–1216.

Kim S, Kim D, Cho S, Kim J, Kim J-S. 2014. Highly efficient RNA-guided genome editing in human cells via delivery of purified Cas9 ribonucleoproteins. *Genome Research* **24**: 1012–1019.

Klinger T. 2015. The role of seaweeds in the modern ocean. *Perspectives in Phycology* **2**: 31–39.

Knight M. 1929. Studies in the Ectocarpaceae. II. The life-history and cytology of *Ectocarpus siliculosus*, Dillw. *Transaction of Royal Society* **LVI**: 307–342.

Kroth PG. 2013. Getting a grip on genetic modification in brown algae. *Journal of Phycology* **49**: 816–818.

La Barre S, Potin P, Leblanc C, Delage L. 2010. The halogenated metabolism of brown algae (Phaeophyta), its biological importance and its environmental significance. *Marine Drugs* **8**: 988–1010.

Li H. 2013. Aligning sequence reads, clone sequences and assembly contigs with BWA-MEM. arXiv:1303.3997 [q-bio].

Lipinska A, Cormier A, Luthringer R, Peters AF, Corre E, Gachon CMM, Cock JM, Coelho SM. 2015. Sexual dimorphism and the evolution of sex-biased gene expression in the brown alga *Ectocarpus*. *Molecular Biology and Evolution* **32**: 1581–1597.

Macaisne N, Liu F, Scornet D, Peters AF, Lipinska A, Perrineau M-M, Henry A, Strittmatter M, Coelho SM, Cock JM. 2017. The *Ectocarpus IMMEDIATE UPRIGHT* gene encodes a member of a novel family of cysteine-rich proteins with an unusual distribution across the eukaryotes. *Development* **144**: 409–418.

McHugh DJ, FAO. 2003. *A guide to the seaweed industry. FAO Fisheries Technical Paper No. 441*. Rome, Italy: FAO.

McKenna A, Hanna M, Banks E, Sivachenko A, Cibulskis K, Kernytsky A, Garimella K, Altshuler D, Gabriel S, Daly M *et al.* 2010. The Genome Analysis Toolkit: a MAPREDUCE framework for analyzing next-generation DNA sequencing data. *Genome Research* **20**: 1297–1303.

Michel G, Tonon T, Scornet D, Cock JM, Kloareg B. 2010a. The cell wall polysaccharide metabolism of the brown alga *Ectocarpus siliculosus*. Insights into the evolution of extracellular matrix polysaccharides in eukaryotes. *New Phytologist* **188**: 82–97.

Michel G, Tonon T, Scornet D, Cock JM, Kloareg B. 2010b. Central and storage carbon metabolism of the brown alga *Ectocarpus siliculosus*: insights into the origin and evolution of storage carbohydrates in eukaryotes. *New Phytologist* **188**: 67–81.

Mignerot L, Nagasato C, Peters AF, Perrineau M-M, Scornet D, Pontheaux F, Djema W, Badis Y, Motomura T, Coelho SM *et al.* 2019. Unusual patterns of mitochondrial inheritance in the brown alga *Ectocarpus*. *Molecular Biology and Evolution* **36**: 2778–2789.

Mikami K. 2014. A technical breakthrough close at hand: feasible approaches toward establishing a gene-targeting genetic transformation system in seaweeds. *Frontiers in Plant Science* **5**: e498.

Montecinos AE, Couceiro L, Peters AF, Desrut A, Valero M, Guillemin M-L. 2017. Species delimitation and phylogeographic analyses in the *Ectocarpus* subgroup *siliculosi* (Ectocarpales, Phaeophyceae). *Journal of Phycology* **53**: 17–31.

Nagasato C, Tanaka A, Ito T, Katsaros C, Motomura T. 2017. Intercellular translocation of molecules via plasmodesmata in the multiseriate filamentous brown alga, *Halopteris congesta* (Sphacelariales, Phaeophyceae). *Journal of Phycology* **53**: 333–341.

Nagasato C, Terauchi M, Tanaka A, Motomura T. 2015. Development and function of plasmodesmata in zygotes of *Fucus distichus*. *Botanica Marina* **58**: 229–238.

Nymark M, Sharma AK, Sparstad T, Bones AM, Winge P. 2016. A CRISPR/Cas9 system adapted for gene editing in marine algae. *Scientific Reports* **6**: e24951.

Oertel W, Wichard T, Weissgerber A. 2015. Transformation of *Ulva mutabilis* (Chlorophyta) by vector plasmids integrating into the genome. *Journal of Phycology* **51**: 963–979.

Ortega A, Geraldi NR, Alam I, Kamau AA, Acinas SG, Logares R, Gasol JM, Massana R, Krause-Jensen D, Duarte CM. 2019. Important contribution of macroalgae to oceanic carbon sequestration. *Nature Geoscience* **12**: 748–754.

Pausch P, Al-Shayeb B, Bisom-Rapp E, Tsuchida CA, Li Z, Cress BF, Knott GJ, Jacobsen SE, Banfield JF, Doudna JA 2020. CRISPR-CasΦ from huge phages is a hypercompact genome editor. *Science* **369**: 333–337.

Peters AF, Marie D, Scornet D, Kloareg B, Cock JM. 2004. Proposal of *Ectocarpus siliculosus* (Ectocarpales, Phaeophyceae) as a model organism for brown algal genetics and genomics. *Journal of Phycology* **40**: 1079–1088.

Peters AF, Scornet D, Ratin M, Charrier B, Monnier A, Merrien Y, Corre E, Coelho SM, Cock JM. 2008. Life-cycle-generation-specific developmental processes are modified in the *immediate upright* mutant of the brown alga *Ectocarpus siliculosus*. *Development* **135**: 1503–1512.

Ritter A, Dittami SM, Goulitquer S, Correa JA, Boyen C, Potin P, Tonon T. 2014. Transcriptomic and metabolomic analysis of copper stress acclimation in *Ectocarpus siliculosus* highlights signaling and tolerance mechanisms in brown algae. *BMC Plant Biology* **14**: e116.

Ritter A, Ubertini M, Romac S, Gaillard F, Delage L, Mann A, Cock JM, Tonon T, Correa JA, Potin P. 2010. Copper stress proteomics highlights local adaptation of two strains of the model brown alga *Ectocarpus siliculosus*. *Proteomics* **10**: 2074–2088.

Savić N, Ringnalda FC, Berk C, Bargsten K, Hall J, Jinek M, Schwank G. 2019. In vitro generation of CRISPR-Cas9 complexes with covalently bound repair templates for genome editing in mammalian cells. *BIO-PROTOCOL* **9**(1).

Serif M, Dubois G, Finoux A-L, Teste M-A, Jallet D, Daboussi F. 2018. One-step generation of multiple gene knock-outs in the diatom *Phaeodactylum tricornutum* by DNA-free genome editing. *Nature Communications* **9**: e3924.

Starr RC, Zeikus JA. 1993. UTEX – The Culture Collection of Algae at the University of Texas at Austin: 1993 list of cultures. *Journal of Phycology* **29** (Suppl.): 1–106.

Sterck L, Billiau K, Abeel T, Rouzé P, Van de Peer Y. 2012. ORCAE: online resource for community annotation of eukaryotes. *Nature Methods* **9**: e1041.

Strittmatter M, Grenville-Briggs LJ, Breithut L, Van West P, Gachon CMM, Küpper FC. 2016. Infection of the brown alga *Ectocarpus siliculosus* by the oomycete *Eurychasma dicksonii* induces oxidative stress and halogen metabolism. *Plant, Cell & Environment* **39**: 259–271.

Suzuki K, Tsunekawa Y, Hernandez-Benitez R, Wu J, Zhu J, Kim EJ, Hatanaka F, Yamamoto M, Araoka T, Li Z *et al.* 2016. *In vivo* genome editing via CRISPR/Cas9 mediated homology-independent targeted integration. *Nature* **540**: 144–149.

Tarver JE, Cormier A, Pinzón N, Taylor RS, Carré W, Strittmatter M, Seitz H, Coelho SM, Cock JM. 2015. MicroRNAs and the evolution of complex multicellularity: identification of a large, diverse complement of microRNAs in the brown alga *Ectocarpus*. *Nucleic Acids Research* **43**: 6384–6398.

Thorvaldsdóttir H, Robinson JT, Mesirov JP. 2013. Integrative Genomics Viewer (IGV): high-performance genomics data visualization and exploration. *Briefings in Bioinformatics* **14**: 178–192.

Wahl M, Molis M, Hobday AJ, Dudgeon S, Neumann R, Steinberg P, Campbell AH, Marzinelli E, Connell S. 2015. The responses of brown macroalgae to environmental change from local to global scales: direct versus ecologically mediated effects. *Perspectives in Phycology* **2**: 11–29.

Zetsche B, Gootenberg J, Abudayyeh O, Slaymaker I, Makarova K, Essletzbichler P, Volz S, Joung J, van der Oost J, Regev A *et al.* 2015. Cpf1 is a single RNA-guided endonuclease of a class 2 CRISPR-Cas system. *Cell* **163**: 759–771.

Zhang Y, Jiang P, Gao J, Liao J, Sun S, Shen Z, Qin S. 2008. Recombinant expression of *rt-PA* gene (encoding Reteplase) in gametophytes of the seaweed *Laminaria japonica* (Laminariales, Phaeophyta). *Science in China Series C: Life Sciences* **51**: 1116–1120.

Supporting Information

Additional Supporting Information may be found online in the Supporting Information section at the end of the article.

Fig. S1 Growth of partheno-sporophyte germlings is inhibited in the presence of 2-Fluoroadenine.

Fig. S2. Normal morphology and reproduction of the *apt fkbp12* double mutant.

Table S1 Sequences of oligonucleotide primers and crRNAs used in this study.

Table S2 Numbers of 2FAR individuals detected in each biolistic or microinjection delivery experiment.

Table S3 Predicted possible off-target sites for all the crRNAs used in this study.

Table S4 Genome-wide analysis of sequence variants in the *apt* mutant Ex1-1.

Please note: Wiley Blackwell are not responsible for the content or functionality of any Supporting Information supplied by the authors. Any queries (other than missing material) should be directed to the *New Phytologist* Central Office.